Solubility of CO_2, CO, and H_2 in the Ionic Liquid [bmim][PF_6] from Monte Carlo Simulations

Ilina Urukova,[†] Johannes Vorholz,[‡] and Gerd Maurer*[,†]

Lehrstuhl für Technische Thermodynamik, University of Kaiserslautern, D-67653 Kaiserslautern, Germany, and DEGUSSA AG, D-63457 Hanau-Wolfgang, Germany

Received: February 21, 2005; In Final Form: May 2, 2005

This work reports predictions from molecular simulation results for the solubility of the single gases carbon dioxide, carbon monoxide, and hydrogen in the ionic liquid 1-*N*-butyl-3-methyl-imidazolium hexafluorophosphate ([bmim][PF_6]) at temperatures from 293 to 393 K and at pressures up to 9 MPa. The predictions are achieved by Gibbs ensemble Monte Carlo simulations at constant pressure and temperature (*NpT*-GEMC). The intermolecular forces are approximated by effective pair potentials for the pure gases and by a quantum-chemistry-based pair potential for [bmim][PF_6]. The interactions between unlike groups are described using common mixing rules without any adjustable binary interaction parameter. The simulation results for the solubility of hydrogen agree within their statistical uncertainty with experimental data, whereas the results for carbon monoxide and carbon dioxide reveal somewhat larger deviations.

1. Introduction

Ionic liquids (ILs) are salts which are liquid at around room temperature. An outstanding characteristic is their nonvolatility. Ionic liquids are good solvents for many substances. Ionic liquids are currently under intensive investigation, as they are assumed to provide a huge potential for applications in various fields, for example, as solvents and catalysts for chemical reactions (e.g., hydrogenation and hydroformylation with respect to the investigated gases H_2 and CO) and separation processes (i.e., in the case of CO_2). Recent studies have proven that catalyst lifetimes can be extended and rates of reaction can be accelerated. Among the other benefits are, for example, their applicability to improve separation and catalyst reuse. The solubility of gases in ionic liquids is an important factor for the design and operation of many processes, and reliable information for this thermodynamic property is necessary. Although numerous experimental studies are available in the literature,[1−16] more data are needed, and their experimental determination is often difficult, tedious, time-consuming, and expensive. Therefore, it is highly desirable to develop predictive methods for estimating the solubility of gases in ionic liquids over a wide range of conditions. In the present work, the Gibbs ensemble Monte Carlo (GEMC)[26,27] molecular simulation technique is employed and tested to predict the solubility of a single gas (carbon dioxide, carbon monoxide, or hydrogen) in a single ionic liquid (1-*N*-butyl-3-methyl-imidazolium hexafluorophosphate ([bmim][PF_6])) from the intermolecular pair potential of the gases and the solvent. The simulations were carried out at constant pressure and temperature. The pair potential models employed in the present study are taken from the literature. The effective pair potential models for the gases (carbon dioxide, the EPM2 potential model by Harris and Yung;[17] carbon monoxide, the three-site model by Straub and Karplus[18] as well the two-center Lennard-Jones model of Bohn et al.;[19] hydrogen, the two-center Lennard-Jones model by Cracknell[21]) were combined with a quantum-chemistry-based pair potential for [bmim][PF_6] (UA1 model by Shah et al.[25]). As the primary goal of the present work is to test the capability of that technique for the prediction of gas solubility, no adjustable binary parameters for interactions between sites on different species were introduced; that is, only common mixing rules without adjustable parameters were employed.

We found a surprisingly good agreement between simulation results and experimental data for the solubility of carbon dioxide and hydrogen in [bmim][PF_6]. The quality of the predictions for the solubility of carbon monoxide in [bmim][PF_6] depends on the particular choice of the pair potential model for carbon monoxide. The prediction results achieved with the model of Bohn et al.[19] agree well with experimental data, whereas large and systematic deviations (in particular at low temperatures) are observed when the pair potential of carbon monoxide is approximated by the model of Straub and Karplus.[18]

2. Simulation Details

2.1. Molecular Models. The EPM2 model proposed by Harris and Yung[17] was selected to describe the intermolecular potential between CO_2 molecules. The EPM2 model approximates carbon dioxide by three sites representing the carbon atom and both oxygen atoms. Each site is the center of a Lennard-Jones potential with an embedded central electrical point charge. The potential parameters were obtained by a scaling procedure,[17] so that the experimental results for the critical point and the vapor−liquid coexistence curve are accurately reproduced. Recent simulations showed that the phase envelope as well as the supercritical isotherm could be reproduced well using the rescaled parameters.[30]

Two different pair potentials were used for carbon monoxide: the three-site model of Straub and Karplus[18] (the SK model) as well as the two-center Lennard-Jones (2CLJ) potential model of Bohn et al.[19] (the BLF model). The SK model combines three Lennard-Jones pair potentials with three partial point charges

* Corresponding author. E-mail: gmaurer@rhrk.uni-kl.de.
[†] University of Kaiserslautern.
[‡] DEGUSSA AG.

10.1021/jp050888j CCC: $30.25 © 2005 American Chemical Society
Published on Web 06/02/2005

which are located on the Lennard-Jones centers (i.e., the carbon and oxygen atoms) and on the center of mass (M site). The BLF model describes the carbon monoxide molecule as a combination of two Lennard-Jones sites (on the carbon as well as on the oxygen atom) without any partial charge. In a preliminary simulation study, both models were tested by simulating the vapor−liquid coexistence curve of carbon monoxide at temperatures from 70 to 120 K and comparing the simulation results with the compilation by Goodwin.[20] That comparison revealed that both pair potential models are equally suited to reproduce the vapor−liquid coexistence data. For the vapor phase density, the average relative deviation between simulation and experiment is about 7% for the SK model and 6% for the BLF model. For the liquid phase density, the two models predict densities that deviate by less than 2% from the experimental results. Furthermore, the average relative deviation between the experimental and the calculated vapor pressures amounted to about 4% for both models. As shown by Straub and Karplus, the SK model is also in accordance with the results of ab initio calculations for the interaction energies between CO and CO on one side and water, formamide, methanol, and imidazole on the other side.

A literature survey resulted in three proposals for the pair potential of hydrogen.[21−23] These proposals were tested in preliminary studies where the density of hydrogen at 0.85 and 10 MPa was determined by computer simulations over the temperature range from 120 to 350 K and compared with the compilation of McCarty et al.[24] The best agreement between the simulation results and the compilation was achieved with the pair potential model of Cracknell.[21] For example, with that model (which was published in 2001), the absolute average deviation between simulation and compilation results for the density was 0.18 kg m^{-3}, whereas it increased to 0.99 and 1.13 kg m^{-3}, respectively, when the older models of Buch (1994)[22] and Dondi et al. (1972)[23] were applied. Cracknell's model for the pair potential of hydrogen is a two-center Lennard-Jones (2CLJ) potential, where each hydrogen is represented by one LJ center.

The pair potential of the ionic liquid [bmim][PF_6] was approximated by a simplification of the quantum-chemistry-based united atom force field (UA1) model proposed by Shah et al.[25] In the UA1 model, all hydrogen atoms of the cation $[bmim]^+$ are incorporated into the carbon atom centers to which they are bonded ("united carbon atoms"). Each such carbon atom carries an electrical charge that was adopted from a methyl or methylene unit. The $[PF_6]^-$ anion is treated as a single interaction site where the fluorine atoms were subsumed into the phosphorus atom. The total electrical charge of the cation and anion was set to be +e and −e, respectively. In addition to the nonbonded contributions, Shah et al. also considered a term to account for intramolecular rotations. However, in the calculations of the present work, this term was omitted. As it was shown by Shah et al.,[25] this model provides a good agreement with experimental data for various volumetric properties, such as the molar volume, the isothermal compressibility, and the thermal expansion coefficient.

All pure component potential parameters are given in Tables 1 and 2. In general, the total interaction energy (u_{ij}) between two molecules and/or ions *i* and *j* with *m* and *n* interaction sites, respectively, is calculated as the sum of Lennard-Jones and Coulomb contributions:

$$u_{ij} = \sum_{a}^{m}\sum_{b}^{n}\left(\frac{1}{4\pi\epsilon_0}\frac{q_i^{a} q_j^{b}}{r_{ij}^{ab}} + 4\epsilon_{ij}^{ab}\left[\left(\frac{\sigma_{ij}^{ab}}{r_{ij}^{ab}}\right)^{12} - \left(\frac{\sigma_{ij}^{ab}}{r_{ij}^{ab}}\right)^{6}\right]\right) \quad (1)$$

TABLE 1: Geometry Data and Potential Parameters of the Molecular Models for Carbon Dioxide, Carbon Monoxide, and Hydrogen

EPM2		SK		BLF		Cracknell	
r_{C-O}/Å	1.149	r_{C-O}/Å	1.128	1.28	r_{H-H}/Å	0.74
σ_O/Å	3.033	σ_O/Å	3.12	3.2717	σ_H/Å	2.59
ϵ_O/k/K	80.507	ϵ_O/k/K	80.063	42.282	ϵ_H/k/K	12.5
σ_C/Å	2.757	σ_C/Å	3.83	3.2717		
ϵ_C/k/K	28.129	ϵ_C/k/K	13.184	42.282		
q_O/e	−0.3256	q_O/e	−0.85			
q_C/e	0.6512	q_C/e	−0.75			
		q_M/e	1.6			

TABLE 2: Potential Parameters and Cartesian Coordinates of the United Atom Model for [bmim][PF_6]

atom	σ_{ii}/Å	ϵ_{ii}/k/K	q_i/e	*x*	*y*	*z*
N_1	3.250	85.394	0.071	0.494	0.183	0.466
N_3	3.250	85.394	0.133	2.518	−0.211	−0.15
C_2	3.880	53.281	0.229	1.414	−0.745	0.325
C_4	3.880	53.281	0.041	1.035	1.382	0.057
C_5	3.880	53.281	0.096	2.298	1.138	−0.325
C_6	3.775	104.036	0.217	3.771	−0.916	−0.437
C_7	3.905	59.295	0.024	−0.889	−0.026	0.943
C_8	3.905	59.295	0.118	−1.904	−0.006	−0.197
C_9	3.905	59.295	0.118	−3.33	−0.219	0.318
C_{10}	3.905	88.039	−0.047	−4.361	−0.202	−0.809
PF_6	4.720	200.616	−1.000	0	0	0

Here, ϵ_0 (=8.8542·10^{-12} C^2 N^{-1} m^{-2}) is the permittivity of vacuum, q_i^{a} is the charge on site a of molecule/ion *i*, r_{ij}^{ab} denotes the distance between sites a and b, and σ_{ij}^{ab} and ϵ_{ij}^{ab} are Lennard-Jones size and energy parameters for interactions between sites a and b located in molecules/ions *i* and *j*, respectively.

For the Lennard-Jones interactions between unlike sites, we adopt the standard Lorentz−Berthelot combining rules;[29] that is, the cross Lennard-Jones size parameter (σ_{ij}^{ab}) is determined by the arithmetic mean of σ_i^{a} and σ_j^{b}:

$$\sigma_{ij}^{ab} = \frac{1}{2}(\sigma_i^{a} + \sigma_j^{b}) \quad (2)$$

but when both sites obey to a carbon dioxide molecule, the geometric mean is used, as proposed by Harris and Yung:[17]

$$\sigma_{ij}^{ab} = \sqrt{\sigma_i^{a}\sigma_j^{b}} \quad (3)$$

The cross energy well depth (ϵ_{ij}^{ab}) is always calculated as the geometric mean of the energy parameters ϵ_i^{a} and ϵ_j^{b}.

$$\epsilon_{ij}^{ab} = \sqrt{\epsilon_i^{a}\epsilon_j^{b}} \quad (4)$$

No adjustable binary interaction parameters were used. The combining rules for the unlike Lennard-Jones size parameters are additionally given in Table 3.

2.2. Simulation Methodology. The Gibbs ensemble Monte Carlo technique[26,27] in the isothermal−isobaric ensemble (*NpT*-GEMC) was employed to simulate the solubility of a single gas in the ionic liquid [bmim][PF_6]. Usually, Gibbs ensemble simulations are performed in two microscopic regions (subsystems) within the bulk phases, away from the interface. Each subsystem is embedded within its own periodic boundary conditions. To guarantee the internal equilibrium of each region, that is, the temperature, pressure, and chemical potentials of all components are equal in the two subsystems, three types of perturbation are applied. The implemented Monte Carlo moves consist of molecule displacements in the subsystems, volume

TABLE 3: Combining Rules Used for the Unlike Lennard-Jones Size Parameter

	CO_2 (EPM2)	CO (SK)	CO (BLF)	H_2 (Cracknell)	[bmim][PF_6] (UA1)
[bmim][PF_6] (UA1)	arithmetic	arithmetic	arithmetic	arithmetic	geometric
CO_2 (EPM2)	geometric				arithmetic
CO (SK)		arithmetic			arithmetic
CO (BLF)			arithmetic		arithmetic
H_2 (Cracknell)				arithmetic	arithmetic

fluctuations, and particle transfer between the two phases. Each type of move was selected randomly but with a fixed probability. Multiple trial insertions of the particles were performed to increase the efficiency of the transfer step, and the energetically most favorable position was selected with its statistical weight (for details, cf. Vorholz et al.[30]). In a typical simulation, the system consisted of 900 particles (500 gas molecules (CO_2, CO, or H_2) and 400 ions) placed in two subsystems with standard periodic boundaries. The Lennard-Jones part of the system energy was calculated with a method proposed by Theodorou and Suter,[28] and the contribution of the electrostatic interactions was computed applying Ewald summation within vacuum boundary conditions (cf. de Leeuw et al.[31]). The runs were started either from a random distribution or from an output configuration of a previous run. An equilibration period of 10−75 million cycles (depending on the studied system as well as the thermodynamic conditions) was followed by a production period of 10−50 million cycles where the ensemble averages of the desired quantities were accumulated. The equilibrium was assumed to be reached when the instantaneously output thermodynamic properties were fluctuating around constant values. The statistical uncertainties of the simulation results were estimated using the block averaging technique; that is, the whole production period was divided into 5−25 (depending on the length of the production period) blocks of equal size, and the standard deviation of the block averages was then calculated.

The ratio of the different moves used in the calculations was the following: 85% probability that a particle displacement in the subsystems is attempted, 1% probability that a volume change of the subsystems is attempted, and 14% probability that a particle transfer between the phases is attempted. The particle for the translational and rotational displacement or transfer step was selected at random. The maximum changes (that means displacement of a selected molecule and volume change) were adjusted to ensure about 35−50% rate of acceptance for the attempted move. Since ionic liquids have no measurable vapor pressure, the concentration of [bmim][PF_6] in the gas phase was neglected; that is, the transfer probability for ions was set to zero in all simulations. This approximation does not change the number of degrees of freedom (following from the Gibbs phase rule), as both the number of equilibrium conditions and the number of intensive variables are reduced by one.

3. Simulation Results and Discussion

3.1. (CO_2 + [bmim][PF_6]) System. The solubility of carbon dioxide in [bmim][PF_6] was simulated in the *NpT*-Gibbs ensemble for the three temperatures 313.15, 353.15, and 393.15 K and for pressures up to 2.5 MPa. The simulation results are given in Table 4 for preset temperature and pressure as the molality of carbon dioxide in [bmim][PF_6]. Table 4 also gives the statistical uncertainty of the simulation results and a comparison with the experimental data by Pérez-Salado Kamps et al.[4] The comparison is also shown in Figure 1. The statistical uncertainty of the simulation results is in a few cases below 5% and also in a few cases beyond 20%. In most cases, however, it is between 5 and 15%. At 353.15 K, the simulation results agree with the experimental data within that statistical uncertainty, except at 0.5 MPa where the simulation result differs from the experimental number by about 30%. The mean relative deviation amounts to only 8%. At 393.15 K, the simulation results are systematically smaller (by about 10−25%) than the experimental data, whereas, at 313.15 K, the simulation results lie systematically (by about 8−30%) above the experimental results. Although the differences between simulation and measurement are in most cases larger than the statistical uncertainty of the simulation results, the agreement is surprisingly good. It is noteworthy to mention that no experimentally obtained information on gas solubility has been implemented into the simulation at any stage. Additionally, Henry's constants

TABLE 4: Simulation Results (sim) for the Solubility of Carbon Dioxide in [bmim][PF_6] and Comparison with the Correlation Results (cor) from Pérez-Salado Kamps et al.[4] [a]

T/K	*p*/MPa	$m_{CO_2}^{(sim)}$/ mol·kg^{-1}	$\Delta m_{CO_2}^{(sim)}$[b]/ mol·kg^{-1}	$m_{CO_2}^{(cor)}$/ mol·kg^{-1}	deviation/%
313.15	0.5	0.353	0.020	0.2694	31
	1.0	0.701	0.042	0.5384	30
	1.5	0.985	0.021	0.8067	22
	2.0	1.204	0.018	1.0739	12
	2.5	1.445	0.042	1.3396	8
353.15	0.5	0.183	0.019	0.1405	30
	1.0	0.306	0.046	0.2801	
	1.5	0.417	0.062	0.4187	
	2.0	0.573	0.091	0.5561	
	2.5	0.695	0.056	0.6925	
393.15	0.5	0.090	0.013	0.0927	
	1.0	0.163	0.018	0.1846	−12
	1.5	0.214	0.053	0.2759	−22
	2.0	0.303	0.030	0.3665	−17
	2.5	0.355	0.082	0.4563	−22

[a] The deviation between simulated and correlated data is reported only when it is larger than the statistical uncertainty of the simulation result. [b] $\Delta m_{CO_2}^{(sim)}$: absolute statistical uncertainty in the molality of carbon dioxide.

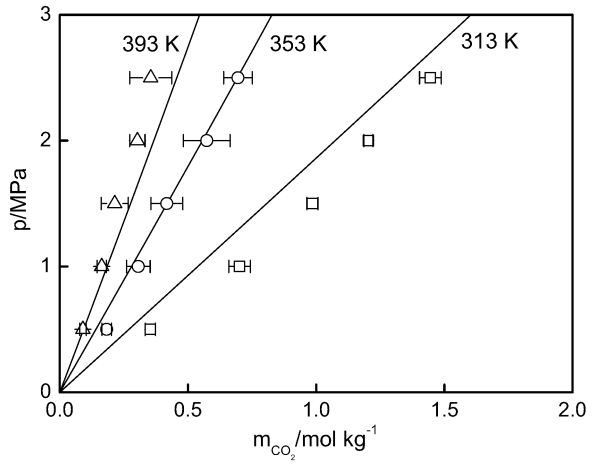

Figure 1. Solubility of CO_2 in the ionic liquid [bmim][PF_6]: comparison between the simulation results (□, ○, △) of this work and the experimental data (—) of Pérez-Salado Kamps et al.[4]

TABLE 5: Henry's Constant of Carbon Dioxide in [bmim][PF_6] (on Mole Fraction Scale) from Molecular Simulations and Experiments

T/K	$k_{H,CO_2}^{(expt)}$/MPa (ref 4)	$k_{H,CO_2}^{(sim)}$/MPa (this work)	$k_{H,CO_2}^{(sim)}$/MPa (ref 32)
298.0	4.71		1.8 ± 0.2
313.15	6.53	5.46 ± 0.49	
323.0	7.86		4.93 ± 1.0
343.0	10.86		6.0 ± 1.5
353.15	12.45	12.27 ± 0.55	
393.15	18.91	22.75 ± 2.23	

for CO_2 in [bmim][PF_6] (on mole fraction) were derived from the simulated solubility data. The results are given in Table 5 and plotted in Figure 2. The difference between the simulation results for Henry's constant of CO_2 in [bmim][PF_6] and the experimental data of Pérez-Salado Kamps et al.[4] is −16% at 313.15 K, −1.4% at 353.15 K, and +20% at 393.15 K. Shah and Maginn[32] recently also published simulation results for Henry's constant of CO_2 in [bmim][PF_6]. Their data are also included in Table 5 and Figure 2. The simulation results of Shah and Maginn are systematically smaller than the experimental data (and the simulation results of the present work). For example, at 298 K, the experimentally determined result for Henry's constant is more than twice the simulation result by Shah and Maginn.

3.2. (CO + [bmim][PF_6]) System. For this binary system, *NpT*-GEMC simulations were carried out at 293.2, 334.05, and 373.15 K at pressures up to 8 MPa for two different combinations of pair potentials. The UA1 model for [bmim][PF_6] was combined either with the SK model or with the BLF model for carbon monoxide. The simulation results are given in Tables 6 (SK model) and 7 (BLF model). For comparison, both tables also give the experimental results for the solubility of carbon monoxide in [bmim][PF_6] as reported recently by Kumełan et al.[13] The comparisons are also shown in Figures 3 and 4. The experimental results reveal that, at temperatures between 293 and 373 K, the solubility of CO in [bmim][PF_6] is nearly independent of temperature. Furthermore, it is much smaller (by a factor of about 10) than the solubility of carbon dioxide in [bmim][PF_6]. The simulation results agree with that experimental finding, but they predict a somewhat stronger influence of temperature.

As it is shown in Figure 3, the combination of the SK model for CO with the UA1 model for [bmim][PF_6] results in a very good agreement between the simulation results and the experimental data for 334.05 K. The mean relative average difference in the liquid phase molality of carbon monoxide is about 5%; that is, it is within the statistical uncertainty of the simulation results, which lie between 9 and 35%. However, the differences are larger both at higher and at lower temperatures. At 373.15 K, the simulation underestimates the molality of carbon monoxide by between 15 and 44%. At 293.2 K, the simulation overestimates the molality of carbon monoxide by between 53 and 66%. These differences are larger than the relative average statistical uncertainty (14% at 293.2 K and 19% at 373.15 K).

Replacing the SK model by the BLF model results in a considerable improvement between simulation results and experimental data for the solubility of carbon monoxide in [bmim][PF_6]. In particular, the combination of the BLF pair potential with the UA1 pair potential gives a less pronounced influence of temperature on the solubility of carbon dioxide. As it is shown in Figure 4, the differences between the simulation results and the experimental results for the liquid phase molality of carbon dioxide at 293.2 K are smaller than

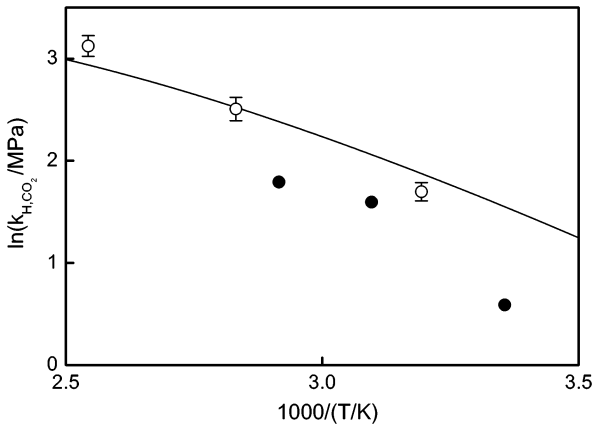

Figure 2. Henry's constant of CO_2 in [bmim][PF_6]: (○) simulation results (and estimated uncertainties) of this work; (●) simulation results of Shah and Maginn;[32] (—) correlated experimental data of Pérez-Salado Kamps et al.[4]

TABLE 6: Simulation Results (sim) for the Solubility of Carbon Monoxide in [bmim][PF_6] by Combining the SK Model with the UA1 Model and Comparison with the Experimental Results (expt) from Kumełan et al.[13] [a]

T/K	p/MPa	$m_{CO}^{(sim)}$/ mol·kg^{-1}	$\Delta m_{CO}^{(sim)}$[b]/ mol·kg^{-1}	$m_{CO}^{(expt)}$/ mol·kg^{-1}	deviation/%
293.2	2.0	0.0575	0.011	0.0347	66
	4.0	0.1075	0.018	0.0690	56
	6.0	0.1539	0.017	0.1009	53
	8.0	0.2049	0.022	0.1319	55
334.05	2.0	0.0394	0.014	0.0355	
	4.0	0.0742	0.012	0.0694	
	6.0	0.0991	0.016	0.1014	
	8.0	0.1375	0.013	0.1321	
373.15	2.0	0.0198	0.005	0.0353	−44
	4.0	0.0565	0.012	0.0694	−19
	6.0	0.0850	0.016	0.1038	−18
	8.0	0.1151	0.017	0.1367	−16

[a] The deviation between simulation and experiment is reported only when it is larger than the statistical uncertainty of the simulation result. [b] $\Delta m_{CO}^{(sim)}$: absolute statistical uncertainty in the molality of carbon monoxide.

TABLE 7: Simulation Results (sim) for the Solubility of Carbon Monoxide in [bmim][PF_6] by Combining the BLF Model with the UA1 Model and Comparison with the Experimental Results (expt) from Kumełan et al.[13] [a]

T/K	p/MPa	$m_{CO}^{(sim)}$/ mol·kg^{-1}	$\Delta m_{CO}^{(sim)}$[b]/ mol·kg^{-1}	$m_{CO}^{(expt)}$/ mol·kg^{-1}	deviation/%
293.2	2.0	0.0400	0.010	0.0347	
	4.0	0.0641	0.014	0.0690	
	6.0	0.0952	0.017	0.1009	
	8.0	0.1409	0.019	0.1319	
334.05	2.0	0.0309	0.007	0.0355	
	4.0	0.0622	0.009	0.0694	
	6.0	0.0920	0.009	0.1014	
	8.0	0.1182	0.015	0.1321	
373.15	2.0	0.0209	0.003	0.0353	−41
	4.0	0.0445	0.009	0.0694	−36
	6.0	0.0936	0.016	0.1038	
	8.0	0.1002	0.015	0.1367	−27

[a] The deviation between simulation and experiment is reported only when it is larger than the statistical uncertainty of the simulation result. [b] $\Delta m_{CO}^{(sim)}$: absolute statistical uncertainty in the molality of carbon monoxide.

15% and well within the statistical uncertainty of the simulation results. At higher temperatures, the molecular simulation underestimates the solubility of carbon monoxide by 9−13% (at 334.05 K) and by 10−41% (at 373.15 K).

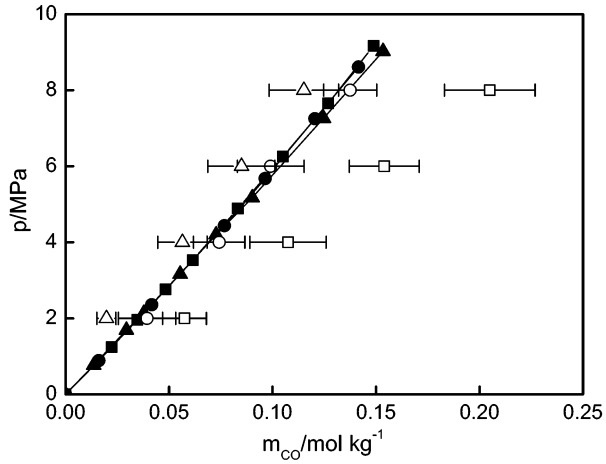

Figure 3. Solubility of CO in the ionic liquid [bmim][PF_6]: comparison between simulation results by employing the SK model [(□) 293.2 K; (○) 334.05 K; (△) 373.15 K] and the experimental data [(−■−) 293.2 K; (−●−) 334.05 K; (−▲−) 373.15 K] of Kumełan et al.[13]

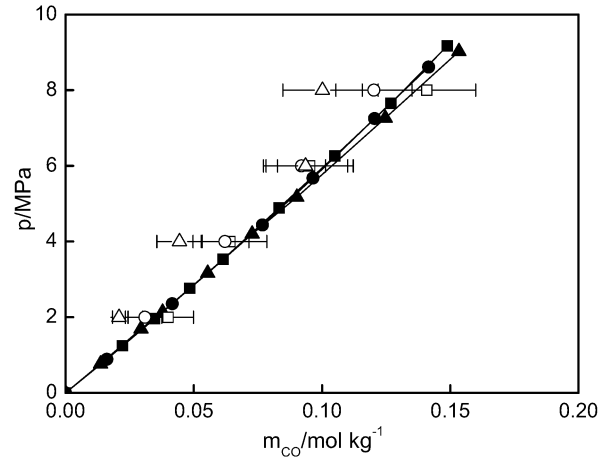

Figure 4. Solubility of CO in the ionic liquid [bmim][PF_6]: comparison between simulation results by applying the BLF model [(□) 293.2 K; (○) 334.05 K; (△) 373.15 K] and the experimental data [(−■−) 293.2 K; (−●−) 334.05 K; (−▲−) 373.15 K] of Kumełan et al.[13]

3.3. (H_2 + [bmim][PF_6]) System. The solubility of hydrogen in [bmim][PF_6] was simulated in the *NpT*-Gibbs ensemble at four temperatures from 313 to 373 K and at pressures up to 9 MPa. The simulation results for the solubility of hydrogen in [bmim][PF_6] (i.e., for the gas molality at preset temperature and pressure) are given and compared to the experimental data of Kumełan et al.[16] in Table 8 and in Figure 5. At 293 K, the solubility (molality) of hydrogen in [bmim][PF_6] is considerably smaller (only about 50%) than the solubility of carbon monoxide. However, at 373 K, the solubility (molality) of both gases is nearly the same (at the same pressure). In contrast to carbon dioxide and carbon monoxide, the solubility of hydrogen in [bmim][PF_6] increases with increasing temperature. The simulation results not only predict this influence qualitatively, but they are also in excellent agreement with the experimental data at all investigated temperatures and pressures. With the exception of a single data point, the predictions for the liquid phase molality of hydrogen agree with the experimental results within the statistical uncertainty of the simulation results (313.05 K, 6−11%; 333.15 K, 6−11%; 353.1 K, 4−9%; 373.15 K, 3−8%). The average (maximum) relative deviation between simulation and experimental data for the molality of hydrogen amounts to 3.7% (4.4%) at 313.05 K, 0.9% (3.3%) at 333.15 K, 0.7% (1.7%) at 353.1 K, and 1.7% (4.6%) at 373.15 K.

TABLE 8: Simulation Results (sim) for the Solubility of Hydrogen in [bmim][PF_6] and Comparison with the Experimental Results (expt) from Kumełan et al.[16] [a]

T/K	*p*/MPa	$m_{H_2}^{(sim)}$/ mol·kg^{-1}	$\Delta m_{H_2}^{(sim)}$[b]/ mol·kg^{-1}	$m_{H_2}^{(expt)}$/ mol·kg^{-1}	deviation/%
313.05	2.0	0.0178	0.0010	0.01720	
	4.0	0.0357	0.0038	0.03428	
	6.0	0.0537	0.0047	0.05139	
	8.0	0.0704	0.0052	0.06831	
333.15	2.0	0.0197	0.0022	0.01903	
	3.0	0.0287	0.0018	0.02856	
	5.0	0.0479	0.0050	0.04766	
	7.0	0.0662	0.0069	0.06626	
	9.0	0.0857	0.0081	0.08541	
353.10	2.0	0.0201	0.0009	0.02095	
	4.0	0.0428	0.0035	0.04214	
	6.0	0.0639	0.0056	0.06323	
	8.0	0.0838	0.0055	0.08369	
373.15	2.0	0.0236	0.0013	0.02312	
	4.0	0.0448	0.0036	0.04653	
	6.0	0.0733	0.0024	0.07011	5
	8.0	0.0981	0.0070	0.09425	

[a] The deviation between simulation and experiment is reported only when it is larger than the statistical uncertainty of the simulation result. [b] $\Delta m_{H_2}^{(sim)}$: absolute statistical uncertainty in the molality of hydrogen.

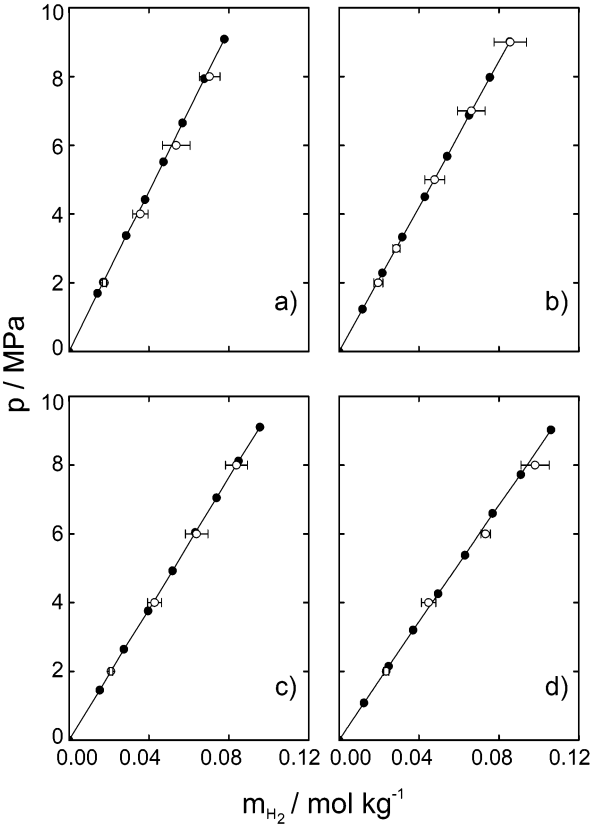

Figure 5. Solubility of H_2 in the ionic liquid [bmim][PF_6]: comparison between the simulation results (○) of this work and the experimental data (−●−) of Kumełan et al.[16] at (a) 313.05 K, (b) 333.15 K, (c) 353.1 K, and (d) 373.15 K.

4. Conclusions

Simulation results for the solubility of three single gases (carbon dioxide, carbon monoxide, and hydrogen) in the ionic liquid [bmim][PF_6] are presented for temperatures from 293 to 393 K and pressures up to 9 MPa and compared with recently published experimental data. Although no interaction parameter was adjusted and therefore the simulation results are truly predictions, there is a good agreement with the experimental

gas solubility data. For the extremely low soluble gas hydrogen, the simulation results for the solubility agree with the experimental data within the statistical uncertainty of the simulation. Although the differences between simulation results and experimental data are somewhat larger for the better soluble gases carbon monoxide and carbon dioxide, the simulation results present reliable estimates for the solubility of these gases in [bmim][PF_6] at temperatures between room temperature and about 400 K, that is, in the temperature range where this ionic liquid is liquid and chemically sufficiently stable. These surprisingly good results encourage the performance of molecular simulation for the prediction of the solubility of (other) gases in (other) ionic liquids to be investigated.

Acknowledgment. Financial support from DFG (Deutsche Forschungsgemeinschaft, Grant Ma 713/41-1) is gratefully acknowledged. The authors express their gratitude to the high performance computing department of the Regionales Hochschulrechenzentrum Kaiserslautern (RHRK) for providing CPU time on its supercomputers.

References and Notes

(1) Blanchard, L. A.; Hancu, D.; Beckman, E. J.; Brennecke, J. F. *Nature* **1999**, *399*, 28.
(2) Blanchard, L. A.; Gu, Z.; Brennecke, J. F. *J. Phys. Chem. B* **2001**, *105*, 2437.
(3) Anthony, J. L.; Maginn, E. J.; Brennecke, J. F. *J. Phys. Chem. B* **2002**, *106*, 7315.
(4) Pérez-Salado Kamps, Á.; Tuma, D.; Xia, J.; Maurer, G. *J. Chem. Eng. Data* **2003**, *48*, 746.
(5) Liu, Z.; Wu, W.; Han, B.; Dong, Z.; Zhao, G.; Wang, J.; Jiang, T.; Yang, G. *Chem.—Eur. J.* **2003**, *9*, 3897.
(6) Scovazzo, P.; Poshusta, J.; DuBois, D.; Koval, C.; Noble, R. *J. Electrochem. Soc.* **2003**, *150*, D91.
(7) Cadena, C.; Anthony, J. L.; Shah, J. K.; Morrow, T. I.; Brennecke, J. F.; Maginn, E. J. *J. Am. Chem. Soc.* **2004**, *126*, 5300.
(8) Ally, M. R.; Braunstein, J.; Baltus, R. E.; Dai, S.; DePaoli, D. W.; Simonson, J. M. *Ind. Eng. Chem. Res.* **2004**, *43*, 1296.
(9) Camper, D.; Scovazzo, P.; Koval, C.; Noble, R. *Ind. Eng. Chem. Res.* **2004**, *43*, 3049.
(10) Scovazzo, P.; Camper, D.; Kieft, J.; Poshusta, J.; Koval, C.; Noble, R. *Ind. Eng. Chem. Res.* **2004**, *43*, 6855.
(11) Marsh, K. N.; Boxall, J. A.; Lichtenthaler, R. *Fluid Phase Equilib.* **2004**, *219*, 93.
(12) Aki, S. N. V. K.; Mellein, B. R.; Saurer, E. M.; Brennecke, J. F. *J. Phys. Chem. B* **2004**, *108*, 20355.
(13) Kumełan, J.; Pérez-Salado Kamps, Á.; Tuma, D.; Maurer, G. *Fluid Phase Equilib.* **2005**, *228−229*, 207.
(14) Ohlin, C. A.; Dyson, P. J.; Laurenczy, G. *Chem. Commun.* **2004**, 1070.
(15) Dyson, P. J.; Laurenczy, G.; Ohlin, C. A.; Vallance, J.; Welton, T. *Chem. Commun.* **2003**, 2418.
(16) Kumełan, J.; Pérez-Salado Kamps, Á.; Tuma, D.; Maurer, G. *J. Pet. Sci. Eng.*, submitted for publication.
(17) Harris, J. G.; Yung, K. H. *J. Phys. Chem.* **1995**, *99*, 12021.
(18) Straub, J. E.; Karplus, M. *Chem. Phys.* **1991**, *158*, 221.
(19) Bohn, M.; Lustig, R.; Fischer, J. *Fluid Phase Equilib.* **1986**, *25*, 251.
(20) Goodwin, R. D. *J. Phys. Chem. Ref. Data* **1985**, *14*, 849.
(21) Cracknell, R. F. *Phys. Chem. Chem. Phys.* **2001**, *3*, 2091.
(22) Buch, V. *J. Chem. Phys.* **1994**, *100*, 7610.
(23) Dondi, M. G.; Valbusa, U.; Scoles, G. *Chem. Phys. Lett.* **1972**, *17*, 137.
(24) McCarty, R. D.; Hord, J.; Roder, H. M. *Selected properties of hydrogen*; NBS Monograph 168; National Bureau of Standards: Washington, DC, 1981.
(25) Shah, J. K.; Brennecke, J. F.; Maginn, E. J. *Green Chem.* **2002**, *4*, 112.
(26) Panagiotopoulos, A. Z. *Mol. Phys.* **1987**, *61*, 813.
(27) Panagiotopoulos, A. Z.; Quirke, N.; Stapleton, M.; Tildesley, D. J. *Mol. Phys.* **1988**, *63*, 527.
(28) Theodorou, D. N.; Suter, U. W. *J. Chem. Phys.* **1985**, *82*, 955.
(29) Allen, M. P.; Tildesley, D. J. *Computer Simulation of Liquids*; Clarendon Press: Oxford, U.K., 1987.
(30) Vorholz, J.; Harismiadis, V. I.; Rumpf, B.; Panagiotopoulos, A. Z.; Maurer, G. *Fluid Phase Equilib.* **2000**, *170*, 203.
(31) de Leeuw, S. W.; Perram, J. W.; Smith, E. R. *Proc. R. Soc. London, Ser. A* **1980**, *A373*, 27.
(32) Shah, J. K.; Maginn, E. J. *Fluid Phase Equilib.* **2004**, *222−223*, 195.